

Exciton-Mechanical Mode Entanglement via Dissipation-Induced Coupling

Eyob A. Sete¹, H. Eleuch², C.H. Raymond Ooi³

¹*Department of Electrical Engineering, University of California, Riverside, California 92521, USA*

²*Department of Physics, McGill University, Montreal, Canada H3A 2T8*

³*Department of Physics, University of Malaya, Kuala Lumpur 50603, Malaysia*

(Dated: October 19, 2019)

We analyze the entanglement between two matter modes in a hybrid quantum system consists of a microcavity, a quantum well, and a mechanical oscillator. Although the exciton mode in the quantum well and the mechanical oscillator are initially uncoupled, their interaction through the microcavity field results in an indirect exciton-mechanical mode coupling. We show that this coupling is a Fano-Agarwal-type coupling induced by the decay of the exciton and the mechanical modes caused by the leakage of photons through the microcavity to the environment. Using experimental parameters and for slowly varying microcavity field, we show that the generated coupling leads to an exciton-mechanical mode entanglement. The maximum entanglement is achieved at the avoided level crossing frequency, where the hybridization of the two modes is maximum. The entanglement is also very robust to the phonon thermal bath temperature.

PACS numbers: 42.50.Wk, 03.65.Ud, 71.36.+c, 78.67.De

Hybrid quantum systems consisting of quantum mechanical oscillators have become a platform for many interesting applications of quantum mechanics. In addition to being a tool to understand the quantum to classical transition, e.g., by creating entanglement between mechanical modes, mechanical oscillators have potential applications in quantum information processing. In this regard, there has been a growing effort in exploiting the mechanical degrees of freedom to engineer devices such as a microwave-to-optical (or vice versa) frequency converter [1, 2] and quantum memory [3, 4]. Moreover, quantum mechanical oscillator has been used as an interface to transfer a quantum state from an optical cavity to a microwave cavity [5, 6]. Interest in merging optomechanical resonators with solid-state systems has been growing; examples include, ultrastrong optomechanical coupling in GaAl vibrating disk resonator [9], cooling of phonons in a semiconductor membrane [10], a strong optomechanical coupling in a vertical-cavity resonator [11], and surface-emitting laser [12]. Coupling a mechanical oscillator to a microcavity that consists of a quantum well has been considered in the context of generating hybrid resonances [13] among photons, excitons, and phonons, and studying the optical bistability [13, 14].

In this work, we analyze the entanglement between the mechanical mode and the exciton mode in a quantum well placed at the antinode of a microcavity that is formed by distributed Bragg reflectors (DBRs). Even though the exciton and the mechanical modes are initially uncoupled, their interaction with a common quantized microcavity field results in an indirect coupling. We show that this coupling is a Fano-Agarwal-type [15, 16] coupling induced by the decay of the exciton and the mechanical mode caused by the leakage of photons through the microcavity to the environment (Purcell effect [17, 18]). We analyze the entanglement in the adiabatic regime, where the damping rate of the microcavity exceeds the cavity-exciton coupling strength. A significant amount

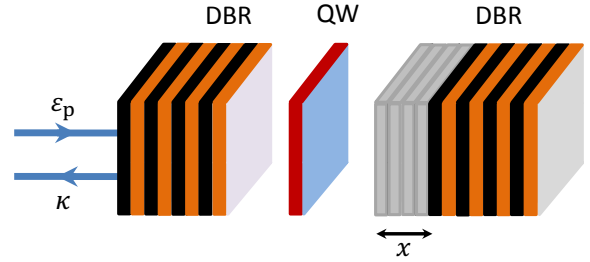


FIG. 1. Schematic of a microcavity made of two sets of distributed Bragg reflectors (DBR) mirrors containing a quantum well (QW) and coupled to a mechanical motion of the mirror. The quantum well is placed at the antinode of the microcavity so that the exciton-cavity mode coupling will be maximum. The black and the orange stripes corresponding to GaAs and AlAs layers, respectively. The microcavity is driven by a pump laser of normalized amplitude ϵ_p and has a damping rate κ . The DBRs are shifted from the equilibrium position due to the radiation pressure force.

of entanglement between the exciton and the mechanical modes can be created at the exciton-mechanical mode hybrid resonance frequencies. We find that the maximum entanglement between the two modes is achieved when the exciton and the mechanical modes hybridization is maximum. Surprisingly, the entanglement persists at high temperature of the phonon thermal bath. Our entanglement analysis is based on realistic parameters from a recent experiment [12].

We consider a microcavity formed by a set of distributed Bragg reflector mirrors and consists of a quantum well placed at the antinode. The microcavity is coupled to the mechanical motion of the mirror via radiation pressure force and to the exciton mode in the quantum well. An exciton in the quantum well can be considered as a quasi-particle resulting from the interaction be-

tween one hole in the valence band and one electron in the conduction band. When the exciton radius is much smaller than the average distance between neighbouring excitons ($\sim n_{\text{ex}}^{-1/2}$ with n_{ex} being exciton concentration), we treat the exciton as a composed boson. In general, in the weak excitation regime, where the density of the excitons is sufficiently low, the interaction between the neighboring excitons due to Coulomb interaction is weak and can be neglected. However, in the moderated driving regime, the interaction between neighbouring excitons becomes strong and nonlinear [19–24], and leads to interesting properties such as squeezing and bistability [25–27]. In this paper we will consider the exciton as a composed boson.

The coupled exciton-optomechanical system is described by the Hamiltonian

$$H = \omega_a a^\dagger a + \omega_{\text{ex}} b^\dagger b + \omega_m c^\dagger c + i\varepsilon_p (a^\dagger e^{-i\omega_p t} - a e^{i\omega_p t}) - g_0 a^\dagger a (c + c^\dagger) + ig(a^\dagger b - ab^\dagger) + \alpha b^\dagger b^\dagger bb. \quad (1)$$

Here the operators a , b , and c are annihilation operators for a photon in the microcavity, an exciton in the quantum well, and a phonon in the mechanical oscillator, respectively. The microcavity is driven by strong drive with frequency ω_p ; ω_a and ω_{ex} are respectively the bare microcavity and exciton frequencies. For the mechanical oscillator, the resonance frequency is ω_m and g_0 is the single-photon optomechanical coupling; g is the linear exciton-cavity mode coupling, and $2\alpha = 6e^2 a_{\text{ex}}/\epsilon A$ [19] is the nonlinear coefficient describing the exciton-exciton scattering due to Coulomb interaction with e , a_{ex} , ϵ , and A being the electron charge, the exciton Bohr radius, the dielectric constant of the quantum well, and the quantization area, respectively. The strong drive of amplitude $\varepsilon_p = \sqrt{\kappa P/\hbar\omega_p}$ with P and κ being the drive laser power and the microcavity damping rate, respectively, leads to a large steady-state optical field in the microcavity which increases the occupation numbers in each mode and the optomechanical coupling. The resulting steady-state intracavity amplitude in turn shifts the equilibrium position of the mechanical oscillator through radiation pressure force.

In a frame rotating with the drive frequency ω_p , the interaction Hamiltonian has the form

$$V = -\Delta_a a^\dagger a - \Delta_{\text{ex}} b^\dagger b + \omega_m c^\dagger c - g_0 a^\dagger a (c + c^\dagger) + ig(a^\dagger b - ab^\dagger) + \alpha b^\dagger b^\dagger bb + i\varepsilon_p (a^\dagger - a), \quad (2)$$

where $\Delta_a = \omega_p - \omega_a$, and $\Delta_{\text{ex}} = \omega_p - \omega_{\text{ex}}$. Using the interaction Hamiltonian Eq. (2), we derive coupled equations for the macroscopic fields, \bar{a} , \bar{b} , and \bar{c} . These equations are obtained by replacing the operators with classical amplitudes in the Heisenberg equations. Using the steady state solutions of the classical equations, we obtain a nonlinear equation for the mean number of excitons I_b in the quantum well: $(I_b/g^2)[(\kappa\gamma/4 + g^2 + \tilde{\Delta}_a \tilde{\Delta}_{\text{ex}})^2 + (\kappa/2\tilde{\Delta}_{\text{ex}} - \gamma\tilde{\Delta}_a/2)^2] = |\varepsilon_p|^2$, where $\tilde{\Delta}_a(I_b) = \Delta_a + 2g_0^2 \bar{n}_\omega/(\omega_m^2 + \gamma_m^2/4)$, and $\tilde{\Delta}_{\text{ex}}(I_b) = \Delta_{\text{ex}} + 2\alpha I_b$.

The nonlinear equation for I_b is a signature that the exciton number can exhibit bistability [13, 14] behaviour for a certain parameter regime. In the following, we discuss exciton-mechanical mode entanglement in the regime where the system is stable.

The nonlinear quantum Langevin equations can be linearized by writing the operators as the sum of the steady state classical mean value plus a fluctuating quantum part: $a = \bar{a}_s + \delta a$, $b = \bar{b}_s + \delta b$, and $c = \bar{c}_s + \delta c$. The linearized Langevin equations of the fluctuation operators then read

$$\delta\dot{a} = -\frac{\kappa}{2}\delta a + i\tilde{\Delta}_a \delta a + g\delta b + G(\delta c + \delta c^\dagger) + \sqrt{\kappa}a_{\text{in}}, \quad (3)$$

$$\delta\dot{b} = -\frac{\gamma}{2}\delta b + i\tilde{\Delta}_{\text{ex}} \delta b - g\delta a - 2i\alpha\bar{b}_s^2 \delta b^\dagger + \sqrt{\gamma}b_{\text{in}}, \quad (4)$$

$$\delta\dot{c} = -\frac{\gamma_m}{2}\delta c + i\omega_m \delta c + G(\delta a^\dagger - \delta a) + \sqrt{\gamma_m}c_{\text{in}}, \quad (5)$$

where $G = g_0\sqrt{\bar{n}_s}$ is the many-photon optomechanical coupling with $\bar{n}_s = |\bar{a}_s|^2$ being the steady state mean photon number in the microcavity. For simplicity, we have chosen the phase of the coherent drive such that $\bar{a}_s = -i|\bar{a}_s|$. Here a_{in} , b_{in} , and c_{in} are the Langevin noise operators for the microcavity, exciton, and the mechanical modes, respectively. All noise operators have zero mean, $\langle a_{\text{in}}(\omega) \rangle = \langle b_{\text{in}}(\omega) \rangle = \langle c_{\text{in}}(\omega) \rangle = 0$. We assume that the microcavity and the quantum well are coupled to a vacuum reservoir and thus the noise operator are delta-correlated: $\langle a_{\text{in}}(\omega)a_{\text{in}}^\dagger(\omega') \rangle = 2\pi\delta(\omega + \omega')$ and $\langle b_{\text{in}}(\omega)b_{\text{in}}^\dagger(\omega') \rangle = 2\pi\delta(\omega + \omega')$. However, the mechanical oscillator is coupled to a thermal bath and the noise operators have the following nonvanishing correlation properties in the frequency domain: $\langle c_{\text{in}}(\omega)c_{\text{in}}^\dagger(\omega') \rangle = 2\pi(n_{\text{th}}+1)\delta(\omega+\omega')$, and $\langle c_{\text{in}}^\dagger(\omega)c_{\text{in}}(\omega') \rangle = 2\pi n_{\text{th}}\delta(\omega+\omega')$, where $n_{\text{th}} = [\exp(\hbar\omega_m/k_B T) - 1]^{-1}$ is the mean number of thermal phonons with k_B being the Boltzmann constant and T the bath temperature.

We next study the entanglement between the exciton and the mechanical modes in the adiabatic regime, where the microcavity damping rate is larger than the exciton-cavity coupling, $\kappa \gg g$, the cavity dynamics reach quasistationary state. We then adiabatically eliminate the cavity mode degrees of freedom by setting $\delta\dot{a} = 0$ in Eq. (3). Substituting the resulting equation into Eqs. (4) and (5), we obtain coupled equations for δb and δc that describe the dynamics of the exciton and the mechanical mode evolutions

$$\delta\dot{b} = -\frac{\Gamma_b}{2}\delta b + i(\tilde{\Delta}_{\text{ex}} - \delta\omega_{\text{ex}})\delta b - 2i\alpha\bar{b}_s^2 \delta b^\dagger - \frac{1}{2}G_{bc}(\delta c + \delta c^\dagger) - \lambda_b a_{\text{in}} + \sqrt{\gamma}b_{\text{in}}, \quad (6)$$

$$\delta\dot{c} = -\frac{\gamma_m}{2}\delta c - i(\omega_m + \delta\omega_m)\delta c - i\delta\omega_m \delta c^\dagger - \frac{1}{2}G_{bc}\delta b + \frac{1}{2}G_{bc}^* \delta b^\dagger + \lambda_c^* a_{\text{in}}^\dagger - \lambda_c a_{\text{in}} + \sqrt{\gamma_m}c_{\text{in}}, \quad (7)$$

where $\Gamma_b = \gamma + \gamma_b$ with $\gamma_b = 4g^2/\kappa[1 + (2\tilde{\Delta}_a/\kappa)^2]$ being the effective relaxation rate of the exciton due to

the damping of photons through the microcavity to the environment, also known as the Purcell effect [17, 18]. Note that the relaxation rate of the exciton is increased by γ_b as result of interaction with the cavity mode; $\gamma_c = 4G^2/\kappa[1 + (2\tilde{\Delta}_a/\kappa)^2]$ is the effective damping rate of the mechanical mode. In contrast to the exciton mode evolution, the cavity-induced relation does not affect the decay term in the Langevin equation for δc , it does however appear in the noise terms as manifested in Eq. (7). Note also that the cavity-exciton coupling shifts the exciton frequency by $\delta\omega_{\text{ex}} = \gamma_b\tilde{\Delta}_a/\kappa$. Similarly, the cavity-mechanical mode coupling gives rise to a shift $\delta\omega_m = 2\gamma_c\tilde{\Delta}_a/\kappa$ in the mechanical mode frequency; $\lambda_{b(c)} = \sqrt{\gamma_{b(c)}}(1 + 2i\tilde{\Delta}_a/\kappa)[1 + (2\tilde{\Delta}_a/\kappa)^2]^{-1/2}$ is the contribution of the cavity-induced dissipation to the noise operator of the exciton (mechanical) mode and finally

$$G_{bc} = \sqrt{\gamma_b\gamma_c} \left(1 + 2i\tilde{\Delta}_a/\kappa\right) \quad (8)$$

is the effective exciton-mechanical mode cross coupling. Notice that the cross coupling depends on the effective decay rates γ_b and γ_c induced by the photon leakage through the microcavity, which is similar to the Fano-Agarwal effect [15, 16]. Dissipation-induced coupling has extensively been explored in quantum optics in creating coherence in three-level atomic systems [30–32]. Here we exploit the dissipation-induced coupling to entangle two matter modes: the exciton and the mechanical modes.

To study the entanglement between the exciton and the mechanical modes, it is more convenient to use the quadrature operators defined by, $\delta x_b = (\delta b^\dagger + \delta b)/\sqrt{2}$, $\delta y_b = i(\delta b^\dagger - \delta b)/\sqrt{2}$, $\delta x_c = (\delta c^\dagger + \delta c)/\sqrt{2}$, and $\delta y_c = i(\delta c^\dagger - \delta c)/\sqrt{2}$ and similar definitions for fluctuation operators $x_{j,\text{in}}, y_{j,\text{in}}$ ($j = a, b$). The equations for these quadrature operators in matrix form read

$$\dot{u} = Ru + \eta, \quad (9)$$

where $u = (\delta x_b, \delta y_b, \delta x_c, \delta y_c)^T$ is vector of quadrature operators and $\eta = (F_{x,\text{in}}^b, F_{y,\text{in}}^b, F_{x,\text{in}}^c, F_{y,\text{in}}^c)^T$ with $F_{x,\text{in}}^b = -\text{Re}(\lambda_b)x_{a,\text{in}} + \text{Im}(\lambda_b)y_{a,\text{in}} + \sqrt{\gamma}x_{b,\text{in}}$, $F_{y,\text{in}}^b = -\text{Re}(\lambda_b)y_{a,\text{in}} - \text{Im}(\lambda_b)x_{a,\text{in}} + \sqrt{\gamma}y_{b,\text{in}}$, $F_{x,\text{in}}^c = \sqrt{\gamma_m}x_{c,\text{in}}$, and $F_{y,\text{in}}^c = -2\text{Re}(\lambda_c)y_{a,\text{in}} - 2\text{Im}(\lambda_c)x_{a,\text{in}} + \sqrt{\gamma_m}y_{c,\text{in}}$. The diffusion matrix R is given by

$$R = \begin{pmatrix} -\frac{\Gamma_b^-}{2} & -\frac{\Delta_{\text{ex}}^+}{2} & \text{Re}(G_{bc}) & 0 \\ \frac{\Delta_{\text{ex}}^-}{2} & -\frac{\Gamma_b^+}{2} & -\text{Im}(G_{bc}) & 0 \\ 0 & 0 & -\frac{\gamma_m}{2} & \omega_m \\ -\text{Im}(G_{bc}) & -\text{Re}(G_{bc}) & -(\omega_m + 2\delta\omega_m) & -\frac{\gamma_m}{2} \end{pmatrix},$$

where $\Gamma_b^\pm = \Gamma_b \pm 4\alpha\text{Im}(\tilde{b}_s^2)$ and $\tilde{\Delta}_{\text{ex}}^\pm = \tilde{\Delta}_{\text{ex}} - \gamma_b\tilde{\Delta}_a/\kappa \pm 2\alpha\text{Re}(\tilde{b}_s^2)$.

We focus on the steady-state entanglement between the exciton and the mechanical modes. For this, one needs to find a stable solution for Eq. (9), so that it reaches a unique steady state independent of the initial conditions. Since we have assumed a_{in} , b_{in} , and

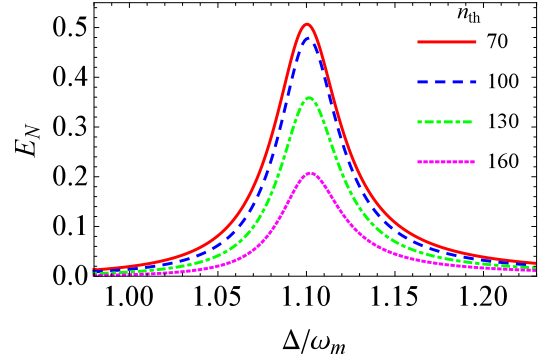


FIG. 2. Logarithmic negativity E_N as a function of the detuning $\Delta = \Delta_{\text{ex}} = \Delta_a$ normalized by the bare mechanical resonance frequency ω_m for the input laser power $P = 24 \mu\text{W}$, and for various values of the thermal phonon number: $n_{\text{th}} = 70$ (red solid curve), 100 (blue dashed curve), 130 (green dot-dashed curve), and 160 (magenta dotted curve). Here we use the experimental parameters from a recent experiment [12] $\kappa = 1/(5\text{ps})$, $\gamma = 1/(0.5\text{ns})$, $\gamma_m = 1/(60\text{ns})$, $g_0/2\pi = 220 \text{ MHz}$, $g/2\pi = 2.4 \text{ GHz}$, and $\omega_m/2\pi = 20 \text{ GHz}$, and $\alpha = 10^{-9}g$.

c_{in} to be zero-mean Gaussian noises and the corresponding equations for fluctuations $\delta x_{j,\text{in}}$ and $\delta y_{j,\text{in}}$ are linearized, the quantum steady state for fluctuations is simply a zero-mean Gaussian state, which is fully characterized by a correlation matrix $V_{ij} = [\langle u_i(\infty)u_j(\infty) + u_j(\infty)u_i(\infty) \rangle]/2$. The solution to Eq. (9) is stable and reaches the steady state when all of the eigenvalues of R have negative real parts. For all results presented in this work, the stability has been checked using the nonlinear equation mentioned earlier. When the system is stable the correlation matrix satisfies Lyapunov equation $RV + VR^T = -D$, where

$$D = \begin{pmatrix} \frac{\Gamma_b}{2} & 0 & 0 & 0 \\ 0 & \frac{\Gamma_b}{2} & 0 & \sqrt{\gamma_b\gamma_c} \\ 0 & \sqrt{\gamma_b\gamma_c} & \frac{\gamma_m}{2}(2n_{\text{th}} + 1) & 0 \\ 0 & 0 & 2\gamma_c + \frac{\gamma_m}{2}(2n_{\text{th}} + 1) & 0 \end{pmatrix}$$

and the elements of the drift matrix D are obtained using the correlations of the noise operators [33] defined earlier. Note that the cavity-induced dissipation terms contribute to the drift matrix. Notably, the off-diagonal element $\sqrt{\gamma_b\gamma_c} = \text{Re}(G_{bc})$ contributes to the correlation between the exciton and the mechanical modes.

In order to quantify the bipartite entanglement, we employ the logarithmic negativity E_N , a measure of bipartite entanglement [34]. For continuous variables, E_N is defined as

$$E_N = \max[0, -\ln 2\chi], \quad (10)$$

where $\chi = 2^{-1/2} [\sigma - \sqrt{\sigma^2 - 4\det V}]^{1/2}$ is the lowest simplistic eigenvalue of the partial transpose of the 4×4 correlation matrix V with $\sigma = \det V_A + \det V_B - 2\det V_{AB}$. Here V_A and V_B represent the exciton and the mechan-

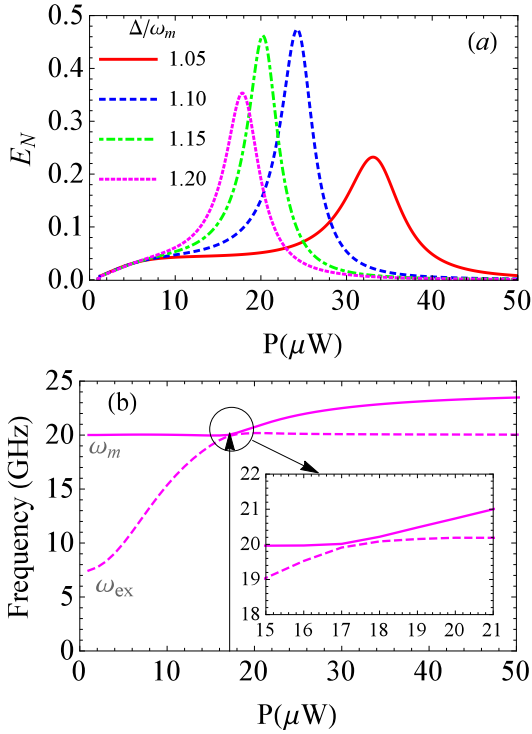


FIG. 3. (a) Logarithmic negativity as a function of the drive laser power P and for different values of the normalized detuning $\Delta/\omega_m = 1.05$ (red solid curve), 1.10 (blue dashed curve), 1.15 (green dot-dashed curve), and 1.20 (magenta dotted curve). Here we used the thermal photon number $n_{th} = 100$. (b) Avoided level crossing between the eigenstates of the exciton-mechanical coupled system for $n_{th} = 100$ and $\Delta/\omega_m = 1.20$. Notice that the maximum entanglement for $\Delta/\omega_m = 1.20$ in (a) appears at the power ($P \approx 17.8 \mu\text{W}$), where the maximum hybridization between the two modes occurs. All the other parameters are as in Fig. 2.

ical modes, respectively, while V_{AB} describes the correlation between the two modes. These matrices are elements of the 2×2 block form of the correlation matrix $V \equiv \begin{pmatrix} V_A & V_{AB} \\ V_{AB}^T & V_B \end{pmatrix}$. The exciton and the mechanical modes are entangled when the logarithmic negativity E_N is positive.

We numerically studied the exciton-mechanical mode entanglement by exploiting the indirect coupling mediated by the cavity field. Using realistic parameters from a recent microcavity experiment [12], we plot in Fig. 2 the logarithmic negativity E_N as a function of the normalized detuning Δ/ω_m and for different values of the thermal phonon occupation number, n_{th} . Here we assumed the exciton-drive and microcavity-laser detuning are the same, $\Delta_a = \Delta_{ex} = \Delta$. Figure 2 reveals that the exciton and the mechanical modes are strongly entangled, a demonstration of entanglement between two matter modes. The maximum entanglement is achieved at frequency where maximum hybridization between the two modes occurs. The entanglement expectedly de-

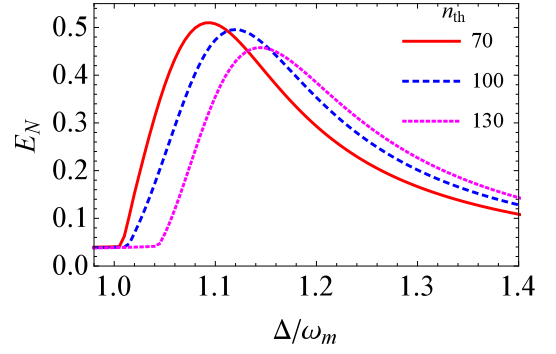


FIG. 4. Logarithmic negativity as a function of the normalized detuning Δ/ω_m optimized over the input laser power P range: 1-50 μW and for different values of the thermal phonon number: $n_{th} = 70$ (red solid curve), 100 (blue dashed curve), and 130 (magenta dotted curve).

creases when the thermal phonon number is increased; however, it persists up to thermal bath phonon number, $n_{th} \lesssim 200$.

In order to study the dependence of the generated entanglement on the applied input laser power, we plot in Fig. 3 the logarithmic negativity versus power for different values of the cavity-laser detuning. As can be seen from this figure, to obtain a maximum entanglement for a given cavity-laser detuning one has to apply a certain laser power strength. Naively, one would expect that an increase in the coupling strength (due to an increase in power) to increase the entanglement. We however find that there exists an optimum amount of power that is needed to obtain the maximum entanglement for the realistic set of parameters [12]. These peaks of the entanglement at different values of the laser power strength and detuning can be explained in terms of the exciton-mechanical mode hybrid resonances. The peaks appear at laser powers where the maximum repulsion between the eigenstates of the two modes occur [see, e.g., Fig. 3 (b)], indicating that the maximum entanglement is achieved at the maximum of hybridization.

The optimized entanglement over the input power as a function of detuning and for different values of the thermal phonon number is shown in Fig. 4. The values of the cavity-laser detuning for which the peaks of the entanglement occur shifts when the thermal phonon numbers are varied. This is because the effective coupling [see Eq. (8)] between the exciton and the mechanical mode depends on the cavity-induced damping rates. These damping rates rely on the number of phonons, thus changing the resonance frequency at which maximum hybridization occurs.

In conclusion, we have analyzed the entanglement between two matter modes (exciton and mechanical modes) in a hybrid quantum system consists of a microcavity, a quantum well, and a quantum mechanical oscillator. We have shown that although the exciton and the mechanical modes are initially uncoupled, their interaction with the

common microcavity field results in dissipation-induced indirect coupling. This indirect coupling is responsible for the entanglement between the exciton and the mechanical modes. Maximum entanglement is achieved in the adiabatic regime where the microcavity damping rate is larger than the coupling strengths and when the two modes form a complete hybridization. Recent successful experiments [9, 10, 12] in coupling mechanical systems with microcavity pave the way for the realization of the proposed entanglement generation between exciton and the mechanical modes via dissipation-induced coupling.

ACKNOWLEDGMENTS

EAS acknowledges support from the Office of the Director of National Intelligence (ODNI), Intelligence Advanced Research Projects Activity (IARPA), through the Army Research Office Grant No. W911NF-10-1-0334. All statements of fact, opinion or conclusions contained herein are those of the authors and should not be construed as representing the official views or policies of IARPA, the ODNI, or the U.S. Government. He also acknowledge support from the ARO MURI Grant No. W911NF-11-1-0268. C. H. R. Ooi acknowledges support from the Ministry of Education of Malaysia through the High Impact Research MoE Grant UM.C/625/1/HIR/MoE/CHAN/04.

-
- [1] T. A. Palomaki, J. W. Harlow, J. D. Teufel, R. W. Simmonds, and K. W. Lehnert, *Nature* **495**, 210 (2013).
 - [2] R. W. Andrews, R. W. Peterson, T. P. Purdy, K. Cicak, R. W. Simmonds, C. A. Regal and K. W. Lehnert, *Nature Phys.* **10**, 321 (2014).
 - [3] S. A. McGee, D. Meiser, C. A. Regal, K. W. Lehnert, and M. J. Holland, *Phys. Rev. A* **87**, 053818 (2013).
 - [4] E. A. Sete and H. Eleuch, *Phys. Rev. A* **91**, 032309 (2015).
 - [5] Y.-D. Wang and A. A. Clerk, *Phys. Rev. Lett.* **108**, 153603 (2012).
 - [6] L. Tian, *Phys. Rev. Lett.* **108**, 153604 (2012).
 - [7] M. Aspelmeyer, T. J. Kippenberg, and F. Marquardt, *Rev. Mod. Phys.* **86**, 1391 (2014).
 - [8] L. Ding, C. Baker, P. Senellart, A. Lemaitre, S. Ducci, G. Leo, and I. Favero, *Phys. Rev. Lett.* **105**, 263903 (2010).
 - [9] L. Ding, C. Baker, P. Senellart, A. Lemaitre, S. Ducci, G. Leo, and I. Favero, *Appl. Phys. Lett.* **98**, 113108 (2011).
 - [10] K. Usami, A. Naesby, T. Bagci, B. Melholt Nielsen, J. Liu, S. Stobbe, P. Lodahl, and E. S. Polzik, *Nat. Phys.* **8**, 168 (2012).
 - [11] S. Anguiano, G. Rozas, A. E. Bruchhausen, A. Fainstein, B. Jusserand, P. Senellart, and A. Lemaitre, *Phys. Rev. B* **90**, 045314 (2014).
 - [12] A. Fainstein, N. D. Lanzillotti-Kimura, B. Jusserand, and B. Perrin, *Phys. Rev. Lett.* **110**, 037403 (2013).
 - [13] E. A. Sete and H. Eleuch, *Phys. Rev. A* **85**, 043824 (2012).
 - [14] O. Kyriienko, T. C. H. Liew, and I. A. Shelykh, *Phys. Rev. Lett.* **112**, 076402 (2014).
 - [15] U. Fano, *Phys. Rev.* **124**, 1866 (1961).
 - [16] G. S. Agarwal, *Quantum Statistical Theories of Spontaneous Emission*, in Springer Tracts in Modern Physics (Springer-Verlag, Berlin, 1976), Vol. 70.
 - [17] E. M. Purcell, *Phys. Rev.* **69**, 681 (1946).
 - [18] E. A. Sete, J. M. Gambetta, and A.N. Korotkov, *Phys. Rev. B* **89**, 104516 (2014).
 - [19] C. Ciuti, P. Schwendimann, B. Deveaud, and A. Quattropani, *Phys. Rev. B* **62**, R4825 (2000).
 - [20] F. Tassone and Y. Yamamoto, *Phys. Rev. B* **59**, 10830 (1999).
 - [21] C. Ciuti, V. Savona, C. Piermarocchi, A. Quattropani, and P. Schwendimann, *Phys. Rev. B* **58**, R10123 (1998).
 - [22] E. Hanamura, *J. Phys. Soc. Jpn* **37**, 1545 (1974).
 - [23] E. Hanamura, *J. Phys. Soc. Jpn* **37**, 1553 (1974).
 - [24] H. Haug, *Z. Phys. B* **24**, 351 (1976).
 - [25] G. Messin, J. Ph. Karr, H. Eleuch, J. M. Courty, and E. Giacobino, *J. Phys. Condens. Matter* **11**, 6069 (1999).
 - [26] A. Baas, J. Ph. Karr, H. Eleuch, and E. Giacobino, *Phys. Rev.* **69**, 023809 (2004).
 - [27] E. A. Sete, H. Eleuch, and S. Das, *Phys. Rev. A*, **84**, 053817 (2011).
 - [28] Y. X. Liu, C. P. Sun, S. X. Yu, and D. L. Zhou, *Phys. Rev. A* **63**, 023802 (2001).
 - [29] H. Eleuch and N. Rachid, *Eur. Phys. J. D* **57**, 259 (2010).
 - [30] V. V. Kozlov, Y. Rostovtsev, and M. O. Scully, *Phys. Rev. A* **74**, 063829 (2006).
 - [31] E. A. Sete, K. E. Dorfman, and J. P. Dowling, *J. Phys. B: At. Mol. Opt. Phys.* **44**, 225504 (2011).
 - [32] E. A. Sete, *Phys. Rev. A* **84**, 063808 (2011).
 - [33] E. A. Sete and H. Eleuch, *Phys. Rev. A* **89**, 013841 (2014).
 - [34] G. Vidal and R. F. Werner, *Phys. Rev. A* **65**, 032314 (2002).